Available online at www.sciencedirect.com

ScienceDirect

www.elsevier.com/locate/jes

JES JOURNAL OF ENVIRONMENTAL SCIENCES

www.jesc.ac.cn

Engineering of responsive polymer based nano-reactors for facile mass transport and enhanced catalytic degradation of 4-nitrophenol

Robina Begum[1], *Zahoor H. Farooqi*[2,*], *Zonarah Butt*[2], *Qingshi Wu*[3], *Weitai Wu*[3], *Ahmad Irfan*[4,5]

1. *Centre for Undergraduate studies, University of the Punjab, New Campus, Lahore 54590, Pakistan*
2. *Institute of Chemistry, University of the Punjab, New Campus, Lahore 54590, Pakistan*
3. *State Key Laboratory for Physical Chemistry of Solid Surfaces, Department of Chemistry, College of Chemistry and Chemical Engineering, Xiamen University, Xiamen 361005, China*
4. *Department of Chemistry, Faculty of Science, King Khalid University, Abha 61413, Saudi Arabia*
5. *Research Center for Advanced Materials Science, King Khalid University, Abha 61413, Saudi Arabia*

ARTICLE INFO

Article history:
Received 14 June 2017
Revised 9 November 2017
Accepted 1 December 2017
Available online 14 December 2017

Keywords:
Polymer microgels
Metal nanoparticles
Hybrid microgels
Catalytic degradation

ABSTRACT

Silver nanoparticles with average diameter of 10 ± 3 nm were synthesized within the sieves of poly(N-isopropylacrylamide-2-hydroxyethylmethacrylate-acrylic acid) (p(NIPAAm-HEMA-AAc)) polymer microgels. Free radial emulsion polymerization was employed for synthesis of p (NIPAAm-HEMA-AAc) polymer microgels. Silver nanoparticles were introduced within the microgels sphere by *in situ* reduction method. Microgels and hybrid microgels were characterized by Fourier transform infrared spectroscopy, ultra violet-visible spectroscopy, transmission electron microscopy and dynamic light scattering measurements. Catalytic activity of Ag-p(NIPAAm-HEMA-AAc) hybrid microgels was studied using catalytic reduction of 4-nitrophenol (4-NP) as a model reaction in aqueous media. The influence of sodium borohydride ($NaBH_4$) concentration, catalyst dose and 4-NP concentration on catalytic reduction of 4-NP was investigated. A linear relationship was found between catalyst dose and apparent rate constant (k_{app}). The mechanism of catalysis by hybrid microgels was explored for further development in this area. The deep analysis of catalytic process reveals that the unique combination of NIPAAm, HEMA and AAc does not only stabilize silver nanoparticles in polymer network but it also enhances the mass transport of hydrophilic substrate like 4-NP from outside to inside the polymer network.

Introduction

Smart microgels have gained much attention owing to their responsive nature. These are extensively used in different fields due to their abilities to respond to the changes occurring in their surroundings (Kumar et al., 2007; Schwall and Banerjee, 2009). Among polymeric microgels, N-isopropylacrylamide (NIPAAm) based microgels are studied widely due to their temperature responsive behavior. This ability of NIPAAm based microgels helps to use them in different fields like in tissue engineering, drug delivery (Schwall and Banerjee, 2009), etalons (Gao et al., 2015) and thermally tunable catalysis (Aditya et al., 2015).

* *Corresponding author. E-mail:* zahoor.chem@pu.edu.pk (Zahoor H. Farooqi).

https://doi.org/10.1016/j.jes.2017.12.003
1001-0742/

Functionalities of NIPAAm based microgels can be enhanced by copolymerizing it with different ionic or non-ionic substances like acrylic acid (Schmidt et al., 2008; Wu et al., 2010) methacrylic acid (Zhou and Chu, 1998), phenyl boronic acid (Farooqi et al., 2011), amines (Zhou et al., 2008), and 2-hydroxyethyl methacrylate (HEMA) (Gan et al., 2009). Acrylic acid is an anionic reagent. It introduces carboxylic acid groups in the microgel network. Snowden et al. (1996) reported the synthesis of N-isopropylacrylamide-co-acrylic acid p(NIPAAm-AAc) microgels and studied the effect of pH, temperature and ionic strength of the medium on their hydrodynamic radius. A comprehensive study was made on the physicochemical properties of the microgels. As microgels are highly cross linked substances so they have the ability to retain their structure even in excess amount of solvent. This property enables us to use these materials as stabilizing or capping agents for the controlled synthesis of metal nanoparticles (Farooqi et al., 2015b). Metal nanoparticles are completely encapsulated within the mesh of microgels thus reducing the chances of formation of metal oxides and also it prevents the agglomeration of metal nanoparticles that is a common practice in case of bare metal nanoparticles (Huang et al., 2012). Li et al. (2006) used p (NIPAAm-AAc) microgels system for the fabrication of CdTe nanocrystals. Perelman et al. (2010) reported the synthesis of p (NIPAM-AAc)/porous SiO_2 hybrid microgels and characterized them using electron microscopy and thin film optical interference spectroscopy. The AAc groups alter the thermoresponsive nature of hybrid microgels at neutral pH and effectively eliminate the lower critical solution temperature. Lu et al. (2006) synthesized the silver-polystyrene/p(N-isopropylacrylamide) (Ag-PS-p(NIPAAm)) hybrid microgels for catalytic reduction of para-nitrophenol (pNP) and reported that catalytic activity can be tuned by varying temperature of the system. This system encounters some problems while dealing with their catalytic applications. Firstly the PS core is solid thus diffusion of reactants as well as products due to presence of core is difficult. This factor reduces the catalytic efficiency of hybrid microgels. Secondly metal nanoparticles were stabilized within the shell made of NIPAAm that contains only amide groups. No negatively charged groups like carboxylic acid groups are present in the network to attract and reside silver ions in the microgel particles. There is a chance of reduction of silver ions outside the network. Silver nanoparticles present outside the network of microgel may aggregate causing reduction in catalytic activity. Moreover contents of silver nanoparticles in the microgels may be small due to absence of electrostatic attractions between functional groups of polymer network and silver ions. We have recently designed Ag-p(NIPAAm-AA) (Farooqi et al., 2015a) and silver-p(N-isopropylacrylamide-methacrylic acid) (Ag-p(NIPAAm-MAA)) (Khan et al., 2013) hybrid microgels to overcome these problems. The acidic components make our system sensitive towards pH along with increasing the ability of microgels to incorporate a large number of silver nanoparticles (Ag NPs). While studying the catalytic activities of hybrid microgels, we worked on pH above or greater than 8. At this pH, all carboxylic groups are ionized thus imparting a net negative charge on the hybrid microgels. p-NP remains in the form of phenolate ion in aqueous medium. This ion also has negative charge. As a result repulsive forces between the phenolate ions and negatively charged carboxylic acid groups of microgels arise which hinder the diffusion of 4-NP towards silver nanoparticles. Moreover size of Ag NPs is increased due to accumulation of a large number of silver ions within the microgels as a result of attraction between positively charged metal ions and negatively charged carboxylate groups (Farooqi et al., 2015a). In these conditions, we need a system that has the ability to overcome above mentioned problems. For this purpose, we have employed HEMA as a second comonomer to synthesize poly(N-isopropylacrylamide-2-hydroxyethyl methacrylate-acrylic acid) (p(NIPAAm-HEMA-AAc)) microgels. In this system concentration of acrylic acid is kept low. The third component overcomes the problem of presence of large number of negatively charged groups as is it a non-ionic component. These microgels have core-shell like structure with high cross-linking density at the core. But advantage of this microgel lies in the fact that core is also formed from the soft microgels network and this enables the reactants and products to diffuse easily through the microgel network. The nonionic monomer HEMA is extensively used for the formulation of drug delivery systems (Yarimkaya and Basan, 2007) and in tissue engineering (Guan et al., 2008) by copolymerizing it with acrylic acid and NIPAAm to form photonic crystals (Honda et al., 2009). Gels based on HEMA are resistant to high temperature and alkaline hydrolysis. Moreover these are less reactive. These groups enhance the hydrophilic nature of microgels (K et al., 2015). Chen et al. (2013) reported the synthesis of microgel colloidal crystals based on NIPAAm, HEMA and acrylic acid and reported the effect of ionic strength and temperature on the stimuli responsive behavior of microgels. To the best of our knowledge microgels based on HEMA were not used as capping agents for metal nanoparticles for their applications in the field of catalysis.

In this paper, we reported the use of microgels composed of NIPAAm, HEMA and acrylic acid as stabilizing agents for Ag nanoparticles as well as nano-reactors for the catalysis of p-NP in aqueous medium. Transmission electron microscopy (TEM), Fourier transform infrared (FTIR) spectroscopy, dynamic light scattering (DLS) and ultraviolet (UV)-Visible studies were employed to characterize the microgels and hybrid microgels. The progress of catalytic reactions was monitored by UV–Visible spectrophotometery.

1. Experimental methods

1.1. *Materials*

NIPAAm, AAc, HEMA, N,N-methylenebis(acrylamide) (BIS), ammonium per sulfate (APS), sodium dodecylsulfate (SDS) and 4-nitrophenol were purchased from Sigma Aldrich. Inhibitor was removed from AAc and HEMA by filtration under reduced pressure. Sodium borohydride ($NaBH_4$) was of analytical grade and was purchased from Scharlau Company. Silver nitrate ($AgNO_3$) was purchased from Germistone Chemicals. Distilled water was used for all solution preparation, synthesis, dialysis and catalytic reduction. Deionized water was used in dynamic light scattering measurements for the analysis of size of microgel particles. The dialysis membrane used for purification of the microgel was Spectra/Por molecular porous membrane

tubing (Fisher Scientific) having molecular weight cut off (MWCO) value 12–14,000.

1.2. Synthesis of p(NIPAAm-co-HEMA-AAc) microgels

The p(NIPAAm-co-HEMA-AAc) microgels were synthesized by free radical emulsion polymerization using NIPAAm (main monomer), HEMA (co-monomer), AAc (co-monomer), BIS (cross linker), APS (initiator), and SDS (surfactant) using strategy reported in literature (Ajmal et al., 2013). 8.5 mmol NIPAAm, 0.8 mmol HEMA, 0.4 mmol AAc, 0.058 g SDS and 0.3 mmol BIS were dissolved in 95 mL distilled water in a 250 mL three necked round bottom flask equipped with nitrogen gas inlet and condenser. It was outfitted with a thermometer. The reaction mixture was stirred and heated to 70°C. After the maintenance of temperature up to 70°C, 5 mL freshly prepared 0.09 mol/L APS solution was added after 30 min which started the process of polymerization. Then the reaction was further preceded for 5 hr under nitrogen purge at constant temperature of 70°C. When initiator was added in the solution, turbidity appeared in the solution that confirmed the onset of polymerization. After the completion of the reaction, the microgels were cooled and were dialyzed using dialysis membrane to remove unreacted monomers, surfactants and initiator. Dialysis was performed for 6 days with daily exchange of water for two times.

1.3. In situ fabrication of silver nanoparticles in p(NIPAAm-co-HEMA-AAc) microgels

Hybrid microgels were synthesized by reduction of silver ions within the framework of p(NIPAAm-co-HEMA-AAc) microgels. 6 mL of the prepared microgels and 29 mL of distilled water were added in a three necked round bottom flask (250 mL) equipped with nitrogen gas inlet and condenser. Then 10 mL freshly prepared $AgNO_3$ (1 mmol/L) solution was added and stirred for 30 min at room temperature. No change in the reaction mixture was observed. Then 0.01 g of $NaBH_4$ dissolved in 5 mL of water was added drop wise into the reaction mixture. The color was rapidly changed after the addition of $NaBH_4$ from milky to orange brown. The pH of the reaction mixture was 4.20 before the addition of $NaBH_4$ and after its addition it changed to 8.75. The reaction mixture was further stirred for 2 hr. Then Ag-p(NIPAAm-HEMA-AAc) hybrid microgels were dialyzed for half an hour against fresh water by using macromolecular porous membrane tubing (Spectra/Por®, Fisher Scientific, USA) having MWCO 12-14,000.

1.4. Catalytic reduction of 4-nitrophenol

Catalytic reduction of 4-NP was investigated with the help of UV–Visible spectrophotometry. 1.6 mL of 4-NP, 0.7 mL $NaBH_4$ and 0.2 mL catalyst were taken in the cuvette. Total volume of the solution was kept 2.5 mL. Spectra were recorded within the range of 250 to 500 nm with a time interval of 1 min until the disappearance of yellow color of the solution. Reduction of 4-NP was performed at different conditions like concentration of $NaBH_4$, amount of catalyst as well as concentration of 4-NP while keeping other parameters constant.

1.5. Characterization studies of microgels and hybrid microgels

FTIR analysis of oven dried samples of microgels and hybrid microgels were carried out on FTIR spectrometer (RX1, Perkin Elmer, USA). Double beam spectrophotometer (UVD-3500, Labomed, USA) was used to characterize Ag nanoparticles fabricated in p(NIPAAm-HEMA-AAc) microgels and to monitor the progress of catalytic reduction of 4-NP. TEM measurements were made on transmission electron microscope (TEM-2100, JEOL, USA) working at accelerating voltage of 120 kV. 10 μL of Ag-p(NIPAAm-HEMA-AAc) hybrid microgels were dried on carbon coated copper grid for analysis of size of Ag nanoparticles fabricated microgels. DLS studies were carried out on dynamic light scattering instrument (B1-200SM, Brookhaven Instruments Corporation, USA) equipped with standard He-Ne laser working at scattering angle of 90°.

2. Results and discussions

2.1. Structural and morphological analysis of pure microgels and hybrid microgels

FTIR spectra of both microgels and hybrid microgels are given in Fig. 1. FTIR spectrum shows no peak at 1600–1650 cm^{-1} that is a characteristic peak for the presence of –C═C– and confirms that polymerization of NIPAAm and other monomers occurred at this position (Ajmal et al., 2013). Absorption peaks in spectra of pure microgels observed at 3273, 1542 and 1638 cm^{-1} represent –N–H (stretching), –N–H (bending) and –C═O vibrations. –N–H stretching peak is broad and intense and it shows that there are some sort of interactions between water molecules and various groups of network of microgel particles. Peaks at 2973 and 2933 cm^{-1} represent asymmetric and symmetric stretching of –C–H bonds of alkanes respectively.

Peaks appeared at 1459 and 1389 cm^{-1} represent $-CH_2$ and $-CH_3$ vibrations respectively. Peak at 1719 cm^{-1} represents the ester carbonyl group (–COO) of HEMA and it confirms the successful incorporation of HEMA into the polymer network.

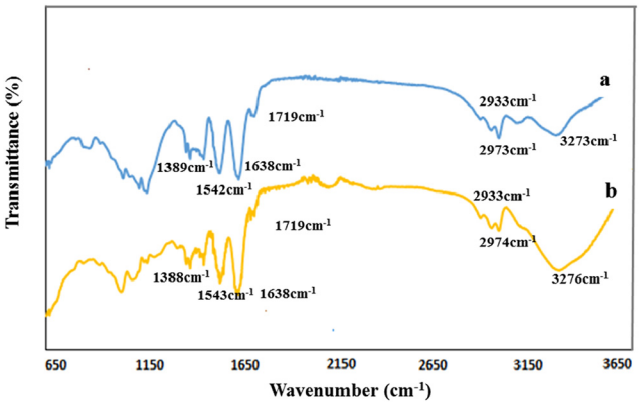

Fig. 1 – Fourier transform infrared (FTIR) spectra of (a) poly(N-isopropylacrylamide-2-hydroxyethylmethacrylate-acrylic acid) (p(NIPAAm-HEMA-AAc)) microgels and (b) silver- poly(N-isopropylacrylamide-2-hydroxyethylmethacrylate-acrylic acid) (Ag-p(NIPAAm-HEMA-AAc)) hybrid microgels.

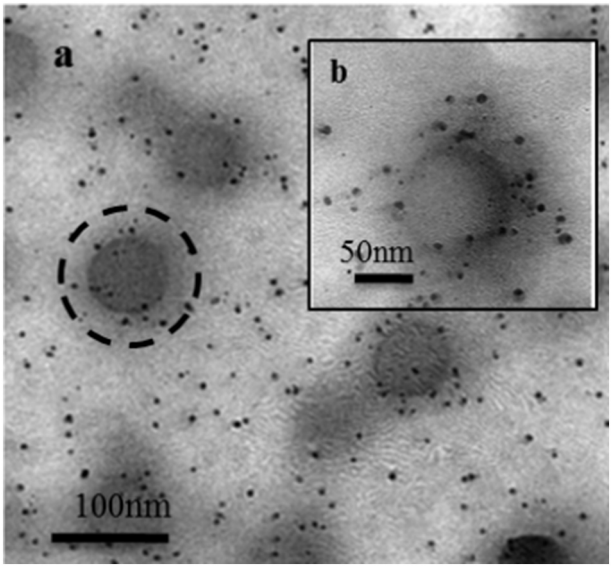

Fig. 2 – (a) Transmission electron microscopic (TEM) images of Ag-p(NIPAAm-HEMA-AAc) hybrid microgels and (b) high resolution TEM images of Ag-p(NIPAAm-HEMA-AAc) hybrid microgels.

From Fig. 1b, we can see that position of peaks is almost same but there is a change in the intensities of the bands and shape of bands. This change in the shapes of peaks occurred due to interactions between the loaded silver nanoparticles and carboxylate groups present in the microgel spheres (Liu et al., 2012).

Morphology of hybrid microgels was further investigated by TEM. TEM images of hybrid microgels are given in (Fig. 2). TEM images indicates core-shell like structure of hybrid microgels due to difference in cross linking density in the inner and outer regions of the microgels (Varga et al., 2001). This difference in cross linking density formed a structure having dense packing within the interior of microgel as compared to peripheral region. The highly cross linked area restricts the incorporation of NPs in the interior region of microgels. Moreover HEMA is more reactive than NIPAAm and AAc due to which core has major portion of HEMA and corona/prefery has major portion of acrylic acid units. So it can be thought that corona region of microgel particles is rich in silver ions before their reduction. Due to high concentration of negative charges in shell region, the Ag NPs are confined in the corona region of microgels while only a small number of NPs is presented in the interior region as shown in Fig. 2b. TEM images show that some silver nanoparticles are also present outside the microgel particles but these were found to be stable. TEM images also reveal the spherical shape of Ag NPs and supported the observations of UV–Visible spectra given in Fig. 3. The average diameter of Ag NPs calculated from TEM images was found to be 10 ± 3 nm (Appendix A Fig. S1).

Incorporation of silver nanoparticles within the microgels was confirmed by the UV–Visible spectroscopy. Fig. 3a shows the UV–Visible spectra of p(NIPAAm-HEMA-AAc) microgels and Ag-p(NIPAAm-HEMA-AAc) microgels. No absorption peak was observed in the UV–Visible spectra of p(NIPAAm-HEMA-AAc) microgels from 200 to 800 nm while a sharp and strong absorption band was observed at 415 nm in hybrid microgels. Pure microgels contain reagents (NIPAAm, HEMA, AAc and BIS) that are UV–Visible inactive, therefore no absorption band was observed in spectra of these microgel particles. The sharp absorption band in hybrid microgels was attributed to the surface plasmon band of Ag NPs. Fig. 3a also confirms the spherical shape of Ag NPs as only single surface plasmon resonance band (λ_{SPR}) was present that is an indication of spherical shape of formed NPs (Gorelikov et al., 2004) as supported by TEM images given in Fig. 2.

UV–Visible spectroscopy was also used to investigate the pH dependent optical properties of Ag-p(NIPAAm-HEMA-AAc) hybrid microgels. UV–Visible spectra of hybrid microgels at 22°C at different pH values are given in Fig. 3b. A red shift in the λ_{SPR} of Ag NPs from 400 to 425 nm was observed with increase in pH of the medium from 2.79 to 11.65. When pH of the medium is low, carboxyl groups are ionized and microgel particles are in shrunken state, thereby restricting ion charge density into a small area (Ajmal et al., 2013). The surrounding medium poorly compensates the restoring forces, thus electrons oscillate at high frequencies and plasmonic coupling occurs at blue region of electromagnetic spectrum (Wu et al., 2009). While at high pH due to ionization of carboxylic groups of AAc, microgels are in swollen state and distance between Ag NPs as well as polarity around Ag NPs increases. Moreover refractive index around the Ag NPs also reduced due to swelling of microgels. All these factors affect the oscillation frequency of Ag NPs (Fernández-López et al., 2012).

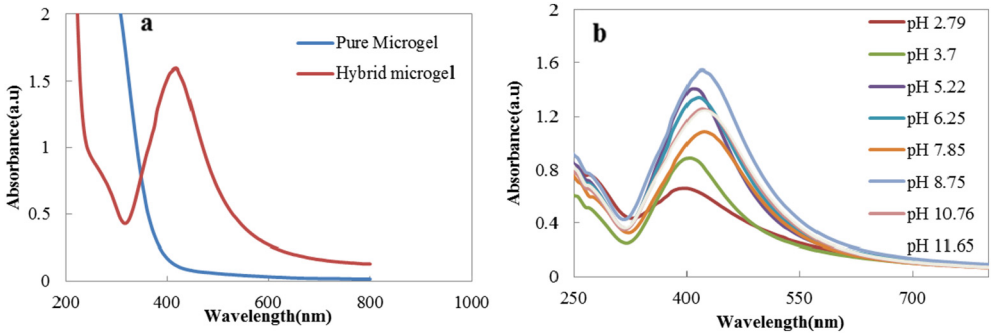

Fig. 3 – Ultraviolet-Visible (UV–Visible) spectra of (a) p(NIPAAm-HEMA-AAc) microgels and Ag-p(NIPAAm-HEMA-AAc) hybrid microgels and (b) Ag-p(NIPAAm-HEMA-AAc) hybrid microgels at 22°C with different pH values.

At high pH silver NPs oscillate slowly with radiations of high wavelength and λ_{SPR} is red shifted. Fig. 3b shows that surface plasmon band of silver nanoparticles can be tuned under various conditions of pH from acidic to highly basic. With increase in acidity of the medium there occurs a decrease in the absorbance of hybrid microgels. The silver nanoparticles stabilized by carboxylate ions present in the microgel networks released from the hybrid microgels at low pH. Because at pH below the pK_a of acrylic acid, all the carboxylate ions gets protonated and could not strongly hold the Ag NPs within the sphere of microgels. Even at extremely low pH values λ_{SPR} is not disappeared that shows the stability of these hybrid systems to be employed as optical sensors.

2.2. Swelling properties of pure and hybrid microgels

Fig. 4 gives pH dependence of hydrodynamic radius of the pure and hybrid microgels. p(NIPAAm-HEMA-AAc) microgels showed a decrease in radius from 155.6 to 39.5 nm when pH was reduced from 8 to 2 respectively. This change in size of microgels can be attributed to pH responsive nature of acrylic acid units of microgels. At low pH values, all the carboxylate groups are protonated and as a result microgel particles remain in de-swollen state. When pH of the external medium exceeds the pK_a of the acrylic acid (pK_a ~4.35) (Farooqi et al., 2015b), carboxylate ions are formed due to deprotonation. These ions increase the hydrophilic behavior of the microgels and water rushes into the microgel network thereby increasing the size of microgel particles. This swelling can be attributed to the development of columbic repulsive forces between the negatively charged carboxylate groups produced as a result of deprotonation of carboxylic acid groups of acrylic acid units. Strong hydrogen bonding between carboxylate ions and polar water molecules holds water molecules within the network of microgels and maintains microgels in swollen state. So size and swelling of these synthesized microgels depend upon the pH of the external medium. It is depicted from Fig. 4 that incorporation of silver nanoparticles within the microgels strongly influences the size of microgels while behavior of response towards change in pH remains the same. The decrease in size of microgel particles on loading of Ag NPs occurs due to donor–acceptor interactions between

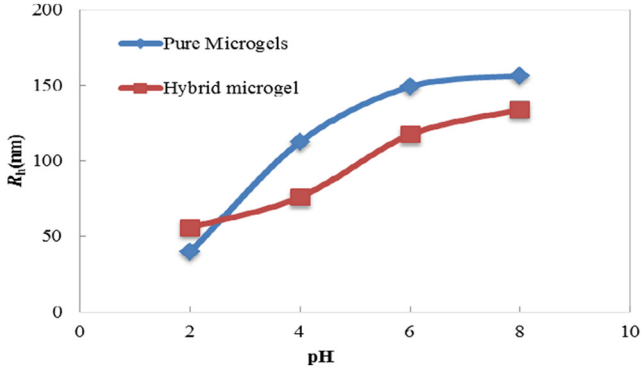

Fig. 4 – Hydrodynamic radius (R_h) of p(NIPAAm-HEMA-AAc) microgels and Ag-p(NIPAAm-HEMA-AAc) hybrid microgels as a function of pH of the medium at 22°C in aqueous medium.

carboxylate groups of microgels and silver nanoparticles and it reduces the chain mobility. Dong et al. (2007) reported that the oxygen of carbonyl groups has a higher binding energy component that is balanced by a corresponding increase in the lower-binding energy components of Ag NPs. As a result a charge transfer phenomena occurs from carbonyl groups towards silver nanoparticles thus increasing the stability of hybrid microgels. This factor reduces the ability of hybrid microgels to swell freely at lower temperature and high pH of the media and causes decrease in the particles size. Pich et al. (2006) had reported the shrinking behavior of microgel particles on fabrication of gold nanoparticles.

As the microgels are swollen at pH above 8, that is why synthesis of hybrid microgels, as well as all the catalytic reactions are carried out at high pH values. As in swollen state, it is feasible for the reactants to diffuse freely inside the sieves of the microgels towards catalyst due to permeable networks.

2.3. Stability of hybrid microgels

Stability of Ag NPs within microgels was investigated by UV–Visible spectroscopy. Hybrid microgels were scanned from time to time at 22°C after their synthesis as shown in Fig. 5a. Fig. 5a shows the spectra of hybrid microgels taken at different time intervals and it indicates that no change occurs in the surface plasmon band of Ag NPs, although a small decrease in the absorbance was observed. This long term stability of Ag NPs shows that strong intermolecular interactions are present between the various groups of microgels and nanoparticles. A charge transfer phenomena occurred between negatively charged carbonyl groups of microgels and inorganic Ag NPs. This factor increases the stability of NPs within microgel sieves (Dong et al., 2007).

As the hybrid microgels reported here are pH sensitive due to the presence of acrylic acid units in the polymer network. It is depicted from Fig. 4 that hybrid microgels are in fully swollen state at pH around 8. Since catalytic reduction of 4-NP is generally carried out in basic medium (Ajmal et al., 2013; Farooqi et al., 2015a; Wunder et al., 2010). Moreover, the pH of the medium increases with the progress of reaction due to the conversion of 4-NP into more basic species 4-aminophenol (4-AP). There is a chance of leaching out of silver nanoparticles from polymer network due to its swelling as a result of increase in pH of the medium during catalysis. So it is necessary to study the effect of pH of the medium on the stability of Ag NPs incorporated in p(NIPAAm-HEMA-AAc). Therefore, the stability of Ag-p(NIPAAm-HEMA-AAc) hybrid microgels was studied at two extreme pH values. Hybrid microgels were scanned immediately after maintaining pH of the medium at 3.7 and 11.65 and after 24 hr. It is depicted from Fig. 5b that hybrid microgels are stable at pH 11.65 as no change in the λ_{SPR} of Ag NPs occurs at this pH. When pH of the medium is low (pH = 3.7), surface plasmon band is observed at 405 nm but this band disappeared after 24 hr. Actually when pH of the medium is lower than that of pK_a of acidic co-monomer, microgels deswell and silver nanoparticles moves out from the sieves of the microgels. This effect causes aggregation as well as oxidation of Ag NPs and hybrid microgels become unstable. As a result, no plasmonic coupling

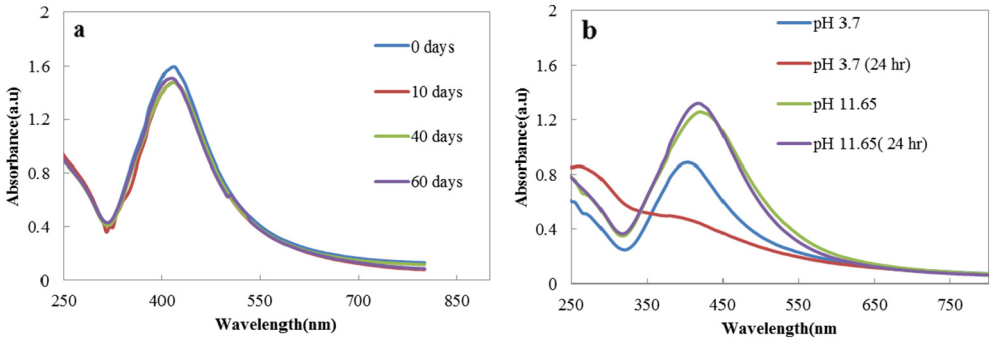

Fig. 5 – UV–Visible spectra of (a) Ag-p(NIPAAm-HEMA-AAc) hybrid microgels at different time intervals at pH of 8.75 and temperature of 22°C and (b) hybrid microgels at room temperature at pH = 3.7 and at pH = 11.65 after 24 hr.

occurs between oscillating electrical field of Ag NPs and electromagnetic radiations and λ_{SPR} disappeared. So, we can conclude that hybrid microgels are stable at high pH values while unstable at lower pH values for long term storage.

2.4. *Catalytic reduction of 4-NP by Ag-p(NIPAAm-HEMA-AAc) hybrid microgels*

Catalytic properties of Ag NPs stabilized in p(NIPAAm-HEMA-AAc) microgels were investigated using reduction of 4-NP in the presence of hybrid microgels in aqueous medium. Reduction of 4-NP to 4-AP on surface of metal NPs is a model reaction as only one product is formed as a result of reduction. The substrate solution is yellow in slightly basic aqueous medium so catalytic reduction can be studied by UV–Visible spectrophotometry as shown in Fig. 6a. Nitrophenolate ion absorbs at 400 nm (Pich et al., 2006) with a strong absorption peak while product of reduction (4-AP) absorbs at 300 nm with a weak absorption band. As only two isosbestic points are present in the spectra so no by products are formed during the reduction of 4-NP to 4-AP by hybrid microgels. Although substrate specie as well as catalyst (hybrid microgels) both absorbs almost in the same region, but study of absorbance measurements at 400 nm for reduction of 4-nitrophenol was not affected by the presence of catalyst as very small amount of catalyst was employed for catalytic reduction during the reaction. Reduction of 4-NP was monitored continuously with the time interval of one minute by UV–Visible spectrophotometry. A gradual decrease in the concentration of 4-NP was observed with decrease in the absorbance peak at 400 nm with time. This decrease in the absorbance at 400 nm was due to catalytic effects of Ag NPs stabilized in p(NIPAAm-HEMA-AAc) microgels. Reaction was also monitored as a controlled reaction in the absence of catalyst for 25 min as shown in Fig. 6b. No change in the absorbance peak at 400 nm was observed although a large amount of $NaBH_4$ was employed. Reduction of 4-NP is favorable thermodynamically in the presence of excess amount of $NaBH_4$ but it is kinetically hindered. A large kinetic barrier is present between electrons donor and accepter species and it reduces the feasibility of the reaction (Saha et al., 2009). As a result the kinetic barrier does not permit the reaction to occur with time only in the presence of $NaBH_4$ (Venkatesham et al., 2014). This kinetic barrier is overcome by the use of Ag NPs given as catalyst. Silver NPs provide a surface for the reaction to occur.

Both reactants 4-NP and BH_4^{-1} get adsorbed on the surface of Ag NPs. Transfer of electron from donor (BH_4^{-1}) to accepter (4-NP) occurs on the surface of the NPs and reduction of the substrate proceeds further that is monitored by change in color from yellow to colorless (Aditya et al., 2015). As we know that concentration and absorbance are directly related to each other. So ratio of absorbance at the start of reaction to the absorbance at any time (A_o/A_t) will be equal to the ratio of initial concentration of 4-NP to that at any time t (C_o/C_t).

When excess amount of $NaBH_4$ is employed, rate of reaction can be considered as independent of the concentration of $NaBH_4$ and follow a pseudo first order kinetics.

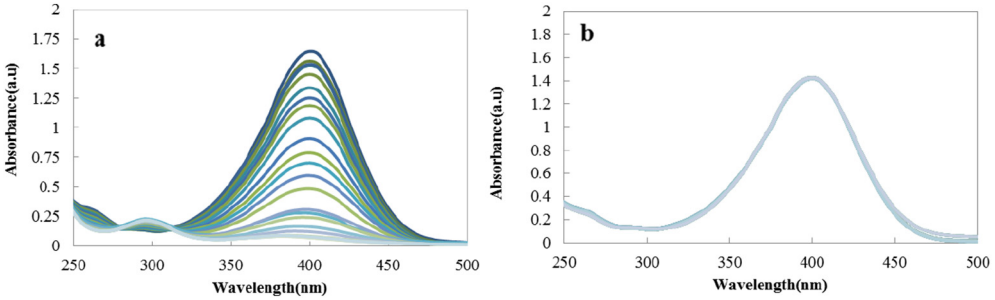

Fig. 6 – UV–Visible spectra for reduction of 4-nitrophenol (4-NP) (a) in the presence of catalyst (0.08 mmol/L 4-NP, 40 μg/mL catalyst, and 6 mmol/L $NaBH_4$) and (b) in the absence of catalyst (0.08 mmol/L 4-NP and 26 mmol/L $NaBH_4$).

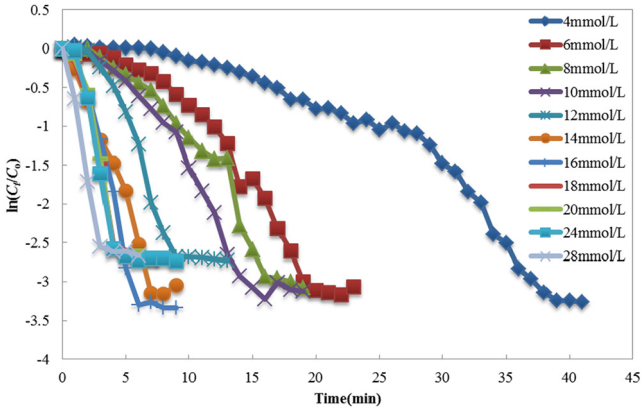

Fig. 7 – Plots of $\ln(C_t/C_o)$ vs. time for different concentrations of $NaBH_4$. Reaction conditions: 40 μg/mL catalyst and 0.08 mmol/L 4-NP.

Catalytic reduction of 4-NP by Ag-p(NIPAAm-HEMA-AAc) microgels was studied under different conditions like concentration of $NaBH_4$, amount of catalyst and concentration of 4-NP as given below.

Dependence of apparent rate constant (k_{app}) on the concentration of $NaBH_4$ was studied by carrying out the reduction at different concentrations of $NaBH_4$. Fig. 7 shows the plots of $\ln(C_t/C_o)$ as a function of time for different concentrations of $NaBH_4$ while concentration of 4-NP and catalyst dose was kept constant. A delay time in the reduction of 4-NP was observed at low concentrations of $NaBH_4$. This time is termed as induction period (Farooqi et al., 2015b). This is the time required for the diffusion of reactants from outside to inside microgels towards the surface of Ag NPs. This time can also be termed as the time required for activating the surface of the metal catalyst by removing oxide layer. This induction time is reduced and finally disappeared as the amount of $NaBH_4$ is increased in the reaction medium as shown in Fig. 7 due to fast regeneration of the surface and quick removal of oxide layers from surface of NPs. Values of k_{app} at different molar ratios of $NaBH_4$ and 4-NP were determined from Appendix A Fig. S2.

With changing the molar concentration of reductant, values of k_{app} were also found to be changed as given in Table 1. Relationship between k_{app} verses concentration of $NaBH_4$ is given in Appendix A Fig. S3. From Appendix A Fig. S3 we can see that with increase in the concentration of $NaBH_4$, the value of k_{app} also increases up to a certain limit and then it becomes constant and we can say that the rate of reaction becomes independent of the concentration of $NaBH_4$. At start, k_{app} increases with increasing concentration of $NaBH_4$ due to increase in the number of BH_4^{-1} ions. These borohydride ions get adsorbed on the surface of NPs along with 4-NP without any competition and rate of reaction increases linearly. When concentration of $NaBH_4$ was higher than 20 mmol/L in the reaction medium, the rate of reaction becomes independent upon its concentration due to the presence of a large number of BH_4^{-1} ions. At this high concentration, the rate of reaction becomes independent for variable concentrations of $NaBH_4$ and the reaction is supposed to a pseudo first order. The value of first order apparent rate constant can be determined using following first order kinetic equation

$$\ln\left(\frac{C_t}{C_o}\right) = -k_{app}t \quad (1)$$

Further studies of the effect of dose of catalyst and concentration of 4-NP were carried out in this region of $NaBH_4$ concentrations.

The effect of concentration of 4-NP on k_{app} is shown in Appendix A Fig. S4. It can be predicted from Appendix A Fig. S4 that the initial value of k_{app} increases with increase in concentration of 4-NP in the range of 0.07 to 0.08 mmol/L. It can be seen from the Table 1 that with further increase in the concentration of 4-NP from 0.08 mmol/L to onward value of rate constant starts to decrease. This behavior can be attributed towards the diffusion of the 4-NP towards the surface of metal nanoparticles. The rate of electron transfer on the surface of metal nanoparticles is affected by different factors like diffusion of 4-NP towards the surface of Ag NPs, interfacial electron transfer and the diffusion of 4-AP away from the Ag NPs (Chang and Chen, 2009; Esumi et al., 2004). The observed rate constant can be expressed as (Graetzel and Frank, 1982):

$$\frac{1}{k_{app}} = \left(\frac{1}{4\pi R^2}\right)\left[\frac{1}{k_{et}} + \frac{R}{D}\right] \quad (2)$$

In this equation R represents the radius of Ag NPs, D is the diffusion coefficient of the reactant while k_{et} is the electron transfer rate constant. Ag NPs possess higher redox potential due to their small size and can accelerate the electron transfer. Thus the phenomenon of heterogeneous charge transfer is faster than the diffusion for the Ag NPs catalyzed reduction of 4-NP by $NaBH_4$ under high concentration of 4-NP. Eq. (2) can be reduced to the Smoluchowski equation given below:

$$k_{app} = 4\pi DR \quad (3)$$

The value of k_{app} is proportional to the diffusion coefficient, while the diffusion coefficient is inversely proportional to the concentration of the 4-NP (Chang and Chen, 2009). With the increase in the concentration of 4-NP, the amount of reactant molecules increases in the reaction medium. Thus the diffusion of 4-NP towards the surface of Ag NPs is hindered that results in a decrease in the value of apparent rate constant (Chiou et al., 2013).

The effect of catalyst dose on the reduction of 4-NP was studied by using different amounts of catalyst as given in Table 1.

The value of k_{app} was determined under various concentrations of catalyst while concentration of 4-NP and $NaBH_4$ was kept constant during all the reactions. It is clearly depicted from Appendix A Fig S5 that catalyst had a significant effect on the value of k_{app}. Calculated values of k_{app} for reduction of 4-NP are 0.354, 0.517, 0.595, 0.604, 0.672, 0.797 and 0.916 min^{-1} for 32, 36, 40, 44, 48, 52, and 56 μg/mL catalyst respectively. Table 1 shows that value of k_{app} increases with increase in the amount of catalyst. With the increase in the amount of catalyst in the

Table 1 – Reaction conditions, values of apparent rate constant (k_{app}) and intrinsic rate constant (k_{int}) for the reduction of 4-nitrophenol (4-NP) in the presence of silver-poly(N-isopropylacrylamide-2-hydroxyethylmethacrylate-acrylic acid) (Ag-p (NIPAAm-HEMA-AAc)) hybrid microgels at 22°C.

Factors	4-NP (mmol/L)	$NaBH_4$ (mmol/L)	Amount of catalyst (μg/mL)	Apparent rate constant (min^{-1})	Intrinsic rate constant (L/(min·g))
	0.08	4	40	0.158	3.95
	0.08	6	40	0.2329	5.82
	0.08	8	40	0.2151	5.37
	0.08	10	40	0.246	6.15
	0.08	12	40	0.4025	10.06
$NaBH_4$	0.08	14	40	0.441	11.02
	0.08	16	40	0.6638	16.59
	0.08	18	40	0.7917	19.79
	0.08	20	40	0.829	20.72
	0.08	28	40	0.873	21.83
	0.08	24	32	0.354	11.06
	0.08	24	36	0.517	14.36
	0.08	24	40	0.595	14.87
Catalyst	0.08	24	44	0.604	13.72
	0.08	24	48	0.672	14
	0.08	24	52	0.797	15.32
	0.08	24	56	0.916	16.35
	0.07	24	40	0.192	4.8
	0.075	24	40	0.38	9.5
4-NP	0.08	24	40	0.595	14.87
	0.085	24	40	0.432	10.8
	0.09	24	40	0.398	9.95
	0.095	24	40	0.258	6.45

$NaBH_4$: sodium borohydride.

reaction medium, availability of active sites for the adsorption of reactants also increases.

Due to increase in the number of nanoparticles per unit volume of the reaction, large number of reactant molecules can attach on the surface of catalyst and rate of electron transfer between reactant (4-NP) and reductant ($NaBH_4$) increases thus increasing the overall reaction rate (Herves et al., 2012). Pich et al. (2006) also studied the reduction of 4-NP on the surface of Au-NPs stabilized in N-vinylcaprolactum/acetoacetoxyethyl methacrylate (VCL/AAEM) dispersions.

They also reported that with the increase in the amount of microgels and amount of Au content in the microgels, rate of reaction increases. There for the values of rate constant for the reduction of 4-NP must be expressed in terms of intrinsic rate constant (k_{int}) for comparison of our system with previously reported catalytic systems. Value of k_{int} for catalytic reduction of 4-NP in aqueous medium in the presence of silver nanoparticles containing microgels reported here in and in literature were also calculated using following equation:

$$k_{int} = \frac{k_{app}}{\text{mass of catalyst/volume of reaction mixture}} \quad (4)$$

Intrinsic rate constants calculated for our system is given in Table 1. Murugan and Jebaranjitham (2012) reported the reduction of 4-NP on the surface of silver nanoparticles immobilized in poly(styrene) functionalized with poly(vinylimidazole) (PS-PVIm-Ag). The calculated intrinsic rate constant from their system is 0.0061 L/(min·g) (Murugan and Jebaranjitham, 2012). Catalytic activity of Ag-p (NIPAAm) hybrid microgels for the reduction of 4-NP was investigated by Liu et al. (2012). The value of k_{int} at 25°C was 1.2 L/(min·g). Silver nanoparticles fabricated in poly(N-isopropylacryamide-allylacetic acid) (p(NIPAAm-AAA)) has been reported by our groups for the catalytic reduction of 4-NP (Farooqi et al., 2015c). k_{int} calculated from this catalytic system was 3.651 L/(min·g). It can be seen from Table 1 that the values of intrinsic rate constants calculated from our system are higher than these values. The reason is that our system is soft, flexible, hydrophilic and total negative charge is less on this system. Moreover it is easy for reactants and products to diffuse through the flexible core of Ag-p(NIPAAm-HEMA-AAc) hybrid microgels.

3. Conclusions

In this work, stable and well-dispersed silver nanoparticles are synthesized in p(NIPAAm-HEMA-AAc) microgels by *in situ* reduction of precursor salt within microgel dispersion for catalytic reduction of 4-NP in aqueous medium. Synthesized microgels and hybrid microgels were characterized by FTIR, DLS, TEM and UV–Visible measurements. Tuning of λ_{SPR} of Ag NPs by pH of the medium provide basis for development of pH sensors. Catalytic efficiency of Ag NPs encapsulated in p (NIPAAm-HEMA-AAc) microgels is studied by the catalytic reduction of 4-NP. Results indicate that with increase in the amount of catalyst k_{app} increases linearly from 0.354 to 0.916 min^{-1} when amount of catalyst is increased from 32 to 56 μg/mL due to the increase in the available active sites for the reactants to adsorb on the surface of catalyst. The value of

k_{app} for the reduction of 4-NP is maximum at a specific value called optimum concentration of 4-NP. Further increase in concentration of 4-NP causes decrease in value of k_{app} and reaction can be studied as diffusion controlled mechanism. The microgels proved efficient stabilizers for metal nanoparticles as no change in the λ_{SPR} is observed even after 60 days of synthesis of hybrid microgels. The hybrid microgels reported here have a potential to be used as pH sensors along with significant catalytic activity.

Acknowledgement

The authors acknowledge financial support for research from Higher Education Commission Pakistan under National Research Program for Universities (NRPU) (No. 20-3995/WRPU/R&D/HEC/14/1212). A. Irfan would like to express his gratitude to Research Centre for Advanced Materials Science - King Khalid University, Saudi Arabia for support.

Appendix A. Supplementary data

Supplementary data to this article can be found online at https://doi.org/10.1016/j.jes.2017.12.003.

REFERENCES

Aditya, T., Pal, A., Pal, T., 2015. Nitroarene reduction: a trusted model reaction to test nanoparticle catalysts. Chem. Commun. 51, 9410–9431.

Ajmal, M., Farooqi, Z.H., Siddiq, M., 2013. Silver nanoparticles containing hybrid polymer microgels with tunable surface plasmon resonance and catalytic activity. Korean J. Chem. Eng. 30, 2030–2036.

Chang, Y.-C., Chen, D.-H., 2009. Catalytic reduction of 4-nitrophenol by magnetically recoverable Au nanocatalyst. J. Hazard. Mater. 165, 664–669.

Chen, M., Zhou, L., Guan, Y., Zhang, Y., 2013. Polymerized microgel colloidal crystals: photonic hydrogels with tunable band gaps and fast response rates. Angew. Chem. Int. Ed. 52, 9961–9965.

Chiou, J.-R., Lai, B.-H., Hsu, K.-C., Chen, D.-H., 2013. One-pot green synthesis of silver/iron oxide composite nanoparticles for 4-nitrophenol reduction. J. Hazard. Mater. 248, 394–400.

Dong, Y., Ma, Y., Zhai, T., Shen, F., Zeng, Y., Fu, H., et al., 2007. Silver nanoparticles stabilized by thermoresponsive microgel particles: synthesis and evidence of an electron donor-acceptor effect. Macromol. Rapid Commun. 28, 2339–2345.

Esumi, K., Isono, R., Yoshimura, T., 2004. Preparation of PAMAM-and PPI-metal (silver, platinum, and palladium) nanocomposites and their catalytic activities for reduction of 4-nitrophenol. Langmuir 20, 237–243.

Farooqi, Z.H., Wu, W., Zhou, S., Siddiq, M., 2011. Engineering of phenylboronic acid based glucose-sensitive microgels with 4-vinylpyridine for working at physiological pH and temperature. Macromol. Chem. Phys. 212, 1510–1514.

Farooqi, Z.H., Khan, S.R., Begum, R., Kanwal, F., Sharif, A., Ahmed, E., et al., 2015a. Effect of acrylic acid feed contents of microgels on catalytic activity of silver nanoparticles fabricated hybrid microgels. Turk. J. Chem. 39, 96–107.

Farooqi, Z.H., Sakhawat, T., Khan, S.R., Kanwal, F., Usman, M., Begum, R., 2015b. Synthesis, characterization and fabrication of copper nanoparticles in N-isopropylacrylamide based co-polymer microgels for degradation of p-nitrophenol. Mater. Sci-Poland 33, 185–192.

Farooqi, Z.H., Tariq, N., Begum, R., Khan, S.R., Iqbal, Z., Khan, A., 2015c. Fabrication of silver nanoparticles in poly (N-isopropylacrylamide-co-allylacetic acid) microgels for catalytic reduction of nitroarenes. Turk. J. Chem. 39, 576–588.

Fernández-López, C., Pérez-Balado, C., Pérez-Juste, J., Pastoriza-Santos, I., de Lera, Á.R., Liz-Marzán, L.M., 2012. A general LbL strategy for the growth of pNIPAM microgels on Au nanoparticles with arbitrary shapes. Soft Matter 8, 4165–4170.

Gan, T., Zhang, Y., Guan, Y., 2009. *In situ* gelation of P (NIPAM-HEMA) microgel dispersion and its applications as injectable 3D cell scaffold. Biomacromolecules 10, 1410–1415.

Gao, Y., Li, X., Serpe, M.J., 2015. Stimuli-responsive microgel-based etalons for optical sensing. RSC Adv. 5, 44074–44087.

Gorelikov, I., Field, L.M., Kumacheva, E., 2004. Hybrid microgels photoresponsive in the near-infrared spectral range. J. Am. Chem. Soc. 126, 15938–15939.

Graetzel, M., Frank, A.J., 1982. Interfacial electron-transfer reactions in colloidal semiconductor dispersions. Kinetic analysis. J. Phys. Chem. 86, 2964–2967.

Guan, J., Hong, Y., Ma, Z., Wagner, W.R., 2008. Protein-reactive, thermoresponsive copolymers with high flexibility and biodegradability. Biomacromolecules 9, 1283–1292.

Herves, P., Pérez-Lorenzo, M., Liz-Marzán, L.M., Dzubiella, J., Lu, Y., Ballauff, M., 2012. Catalysis by metallic nanoparticles in aqueous solution: model reactions. Chem. Soc. Rev. 41, 5577–5587.

Honda, M., Seki, T., Takeoka, Y., 2009. Dual tuning of the photonic band-gap structure in soft photonic crystals. Adv. Mater. 21, 1801–1804.

Huang, C.-C., Lo, S.-L., Lien, H.-L., 2012. Zero-valent copper nanoparticles for effective dechlorination of dichloromethane using sodium borohydride as a reductant. Chem. Eng. J. 203, 95–100.

K, S.S., Siddaramaiah, Gowda, D.V., Datta, V.M., Srivastava, A., 2015. Formulation and evaluation of pH sensitive poly(acrylic acid-co-hydroxyethyl methacrylate)hydrogels for specific site drug delivery. Pharm. Chem. 7, 35–45.

Khan, S.R., Farooqi, Z.H., Ajmal, M., Siddiq, M., Khan, A., 2013. Synthesis, characterization, and silver nanoparticles fabrication in N-isopropylacrylamide-based polymer microgels for rapid degradation of p-nitrophenol. J. Dispers. Sci. Technol. 34, 1324–1333.

Kumar, A., Srivastava, A., Galaev, I.Y., Mattiasson, B., 2007. Smart polymers: physical forms and bioengineering applications. Prog. Polym. Sci. 32, 1205–1237.

Li, J., Liu, B., Li, J., 2006. Controllable self-assembly of CdTe/poly (N-isopropylacrylamide-acrylic acid) microgels in response to pH stimuli. Langmuir 22, 528–531.

Liu, Y.-Y., Liu, X.-Y., Yang, J.-M., Lin, D.-L., Chen, X., Zha, L.-S., 2012. Investigation of Ag nanoparticles loading temperature responsive hybrid microgels and their temperature controlled catalytic activity. Colloids Surf. A Physicochem. Eng. Asp. 393, 105–110.

Lu, Y., Mei, Y., Drechsler, M., Ballauff, M., 2006. Thermosensitive core–shell particles as carriers for Ag nanoparticles: modulating the catalytic activity by a phase transition in networks. Angew. Chem. Int. Ed. 45, 813–816.

Murugan, E., Jebaranjitham, J.N., 2012. Synthesis and characterization of silver nanoparticles supported on surface-modified poly (N-vinylimidazale) as catalysts for the reduction of 4-nitrophenol. J. Mol. Catal. A Chem. 365, 128–135.

Perelman, L.A., Moore, T., Singelyn, J., Sailor, M.J., Segal, E., 2010. Preparation and characterization of a pH-and thermally responsive poly (N-isopropylacrylamide-co-acrylic acid)/porous SiO_2 hybrid. Adv. Funct. Mater. 20, 826–833.

Pich, A., Karak, A., Lu, Y., Ghosh, A.K., Adler, H.-J.P., 2006. Tuneable catalytic properties of hybrid microgels containing gold nanoparticles. J. Nanosci. Nanotechnol. 6, 3763–3769.

Saha, S., Pal, A., Kundu, S., Basu, S., Pal, T., 2009. Photochemical green synthesis of calcium-alginate-stabilized Ag and Au nanoparticles and their catalytic application to 4-nitrophenol reduction. Langmuir 26, 2885–2893.

Schmidt, S., Hellweg, T., von Klitzing, R., 2008. Packing density control in P (NIPAM-co-AAc) microgel monolayers: effect of surface charge, pH, and preparation technique. Langmuir 24, 12595–12602.

Schwall, C.T., Banerjee, I.A., 2009. Micro-and nanoscale hydrogel systems for drug delivery and tissue engineering. Materials 2, 577–612.

Snowden, M.J., Chowdhry, B.Z., Vincent, B., Morris, G.E., 1996. Colloidal copolymer microgels of N-isopropylacrylamide and acrylic acid: pH, ionic strength and temperature effects. J. Chem. Soc. Faraday Trans. 92, 5013–5016.

Varga, I., Gilányi, T., Meszaros, R., Filipcsei, G., Zrinyi, M., 2001. Effect of cross-link density on the internal structure of poly (N-isopropylacrylamide) microgels. J. Phys. Chem. B 105, 9071–9076.

Venkatesham, M., Ayodhya, D., Madhusudhan, A., Babu, N.V., Veerabhadram, G., 2014. A novel green one-step synthesis of silver nanoparticles using chitosan: catalytic activity and antimicrobial studies. Appl. Nanosci. 4, 113–119.

Wu, W., Zhou, T., Zhou, S., 2009. Tunable photoluminescence of Ag nanocrystals in multiple-sensitive hybrid microgels. Chem. Mater. 21, 2851–2861.

Wu, W., Zhou, T., Berliner, A., Banerjee, P., Zhou, S., 2010. Smart core– shell hybrid nanogels with Ag nanoparticle core for cancer cell imaging and gel shell for pH-regulated drug delivery. Chem. Mater. 22, 1966–1976.

Wunder, S., Polzer, F., Lu, Y., Mei, Y., Ballauff, M., 2010. Kinetic analysis of catalytic reduction of 4-nitrophenol by metallic nanoparticles immobilized in spherical polyelectrolyte brushes. J. Phys. Chem. C 114, 8814–8820.

Yarimkaya, S., Basan, H., 2007. Swelling behavior of poly (2-hydroxyethyl methacrylate-co-acrylic acid-co-ammonium acrylate) hydrogels. J. Macromol. Sci. Pure Appl. Chem. 44, 939–946.

Zhou, S., Chu, B., 1998. Synthesis and volume phase transition of poly (methacrylic acid-co-N-isopropylacrylamide) microgel particles in water. J. Phys. Chem. B 102, 1364–1371.

Zhou, Y., Jiang, K., Chen, Y., Liu, S., 2008. Gold nanoparticle-incorporated core and shell crosslinked micelles fabricated from thermoresponsive block copolymer of N-isopropylacrylamide and a novel primary-amine containing monomer. J. Polym. Sci. A Polym. Chem. 46, 6518–6531.